Ketogenic Diet Ameliorates Lipid Dysregulation in Type 2 Diabetic Mice by Downregulating Hepatic Pescadillo 1

Jielin Zhou
Anhui Medical University
Yao Lu
Anhui Medical University
Yajing Jia
Anhui Medical University
Jing Lu
Anhui Medical University
Zhengxuan Jiang
Anhui Medical University
Keyang Chen (chenkeyang@ahmu.edu.cn)
Anhui Medical University https://orcid.org/0000-0002-7648-2726

Research article

Keywords: Ketogenic diet (KD), β-Hydroxybutyrate (β-HB), PES1, lipid metabolism, inflammation

Posted Date: October 6th, 2021

DOI: https://doi.org/10.21203/rs.3.rs-951448/v1

Version of Record: A version of this preprint was published at Molecular Medicine on January 3rd, 2022.
See the published version at https://doi.org/10.1186/s10020-021-00429-6.

Abstract

Background: Previous reports implied a possible link between PES1 and lipid metabolism. However, the role of PES1 in regulation of T2DM related lipid metabolism and the effect of KD on PES1 have not been reported. The aim of present study is to explore the role of PES1 in effects of ketogenic diet (KD) on diabetic mice and its mediated mechanism.

Methods: Male C57BL/6J and KKA^y mice were fed with standard diet (SD) and KD, respectively. Simultaneously, McArdle 7777 cells were treated by β-hydroxybutyric acid (β-HB), *Pes1* siRNA or *Pes1* overexpression plasmid, respectively. Additionally, liver-conditional knockout (CKO) of *Pes1 in vivo* were used.

Results: We unexpectedly found that hepatic PES1 expression in T2DM patients was markedly elevated, but the elevated PES1 was suppressed by KD feeding in T2DM mice with the reduction of hepatic and plasma triglycerides (TG). In mice with CKO of *Pes1*, the protein levels of p300, SREBP1c, FASN, SCD1, caspase1, NLRP3 and GSDMD were dramatically downregulated in livers, and the plasma and hepatic TG, IL-1β and IL-18 were decreased as well. The similar phenomena were also observed in β-HB and *Pes1* knockdown treated hepatocytes. By contrast, *Pes1* overexpression in cultured hepatocytes showed that these levels were significantly enhanced, which however were reduced under β-HB treatment. Mechanistically, we discovered that β-HB decreased CHOP binding to the *Pes1* promoters, resulting in the downregulation of PES1, thereby reducing PES1 binding to *p300* and *caspase1* promoters. The inhibition of p300 and caspase1 expressions elicited the dramatic suppression of acetylation of SREBP1c *via* its interaction with p300, and the decreased GSDMD levels. Besides, knockdown of *caspase1* also alleviated the TG levels in cultured hepatocytes.

Conclusion: KD may improve lipid dysregulation in type 2 diabetic mice by downregulating hepatic PES1 expression.

Introduction

Type 2 diabetes mellitus (T2DM), resulted from insulin resistance (IR) and pancreatic β-cell dysfunction, is a heterogeneous metabolic disorder (Magliano et al. 2020). And compelling evidence showed that T2DM was accompanied by hypertriglyceridemia-based lipid dysregulation (Zheng et al. 2018; Xu et al. 2018), one of the main factors leading to atherosclerosis and even death (McGuire et al. 2016).

Recently, an interesting dietary pattern, ketogenic diet (KD), has been proposed to attain a remarkable decline of hyperglycemia in T2DM (Abbasi 2018). KD is typically characterized by low carbohydrates (5 to 10% of total caloric intake) and high fat consumption (more than 70% of total caloric intake) (Castellana et al. 2020). Additionally, it was reportedly associated with the remission of numerous adverse health outcomes such as obesity, inflammation, cardiovascular disease and cancer (Gentile et al. 2018; Allen et al. 2014; Yancy et al. 2019; Augustin et al. 2018; Watanabe et al. 2020). One study has documented that the KD could alleviate the hyperglycemia in T2DM through producing ketone bodies

(Abbasi 2018). Ketone bodies approximately consist of 78% β-hydroxybutyric acid (β-HB), 20% acetoacetic acid and 2% acetone (Newman et al. 2017). However, due to the high fat content in KD, there are also studies reporting the bad outcomes by the long-term consumption of KD, including no significant weight loss, lipid accumulation, and liver fibrosis (Ellenbroek et al. 2014; Zhang et al. 2016).Nevertheless, the molecular mechanisms underlying the impact of KD have not been satisfactorily explored.

Currently, we unexpectedly observed that liver pescadillo 1 (PES1) expressions in patients and mice with T2DM were markedly elevated. PES1, also known as pescadillo ribosomal biogenesis factor 1, or NOP7, or YPH1, was originally found in zebrafish embryos (Allende et al. 1996).It is evolutionarily highly conserved and forms a complex with BOP1 and WDR12 (PeBoW complex), which is essential for the assembly of 60S ribosomal subunits, DNA replication, cell cycle progression, etc (Du et al. 2002; Cheng et al. 2019).

PES1 is aberrantly upregulated in various malignant tumors such as breast, ovarian and colon cancers, as well as hepatocellular carcinoma (Cheng et al. 2012; Fan et al. 2018; Li et al. 2013).A considerable number of publications have reported that T2DM with lipid dysregulation is associated with increased incidence and mortality from many cancers (Shlomai et al. 2016; Klil-Drori et al. 2017). And one published study discovered that circular antisense non-coding RNA in the INK4 locus (circANRIL), a prototype of circRNA regulating ribosome biogenesis and conferring atheroprotection, acts as a molecular inhibitor of PES1 by binding at the C-terminal domain of PES1 (Holdt et al. 2016). Collectively, these reports suggested the possible link of PES1 to lipid metabolism under T2DM condition.

In this study, we aimed to evaluate the effects of KD or β-HB on diabetic mice or liver cells *via* downregulating PES1 expression, which may be associated with the amelioration of lipid metabolism *in vivo* and *in vitro*. Thus, a novel mechanism of PES1 mediated lipid metabolism under T2DM condition affected by KD intervention would be explored. Our current study may provide a novel therapeutic target for T2DM management and treatment by KD or PES1 inhibitor.

Materials And Methods

Reagents

β-HB (166898) was bought from Sigma Chemical Co (St. Louis, MO). Triglycerides (TG), total cholesterol (TC), alanine aminotransferase (ALT), aspartate aminotransferase (AST) and β-HB assay kits were from Nanjing Jiancheng Bioengineering Institute (Jiangsu, China). The ELISA kit for insulin was obtained from Jianglai Corp (Shanghai, China). Flag-tag (20543-1-AP), β-actin (66009-1-Ig) and Caspase1 (22915-1-AP) antibodies for western bolting, and PES1 (13553-1-AP) antibody for immunofluorescence were obtained from Proteintech, Chicago, USA. PES-1 (NBP2-55211) antibody for western bolting and SREBP1c antibody (NB600-582) for immunofluorescence were bought from Novus Biologicals. SREBP1c (191857), SCD1 (ab19862) and SREBP2 (ab155017) antibodies for western bolting were purchased from Abcam. FASN (3180S) antibody for western bolting was from Cell Signaling Technology (Beverley, MA). NLRP3 (DF7438) and GSDMD (AF4012) antibodies for western bolting were from Affinity. CHOP (sc-7351), p300

(sc-48343) and Ac-SREBP1c (Acetylated-SREBP1c, sc-13551 AC) antibodies were bought from Santa Cruz Biotechnology. RNAex Pro Reagent (AG21102), reverse transcription kits (AG11707), SYBR Green qPCR SuperMix (AG11718) were bought from Accurate Biology. Cell counting kit-8 (CCK-8) (C0005) was from Target Mol (Shanghai, China). Chromatin immunoprecipitation (ChIP) assay kit (P2078) was purchased from Beyotime. Rat *Pes1* and *caspase1* short interfering RNA (siRNA) and *Pes1* overexpression plasmid were purchased from GENERAL BIOL (Anhui, China).

Human subjects

Normal controls were the 32 subjects with gastric cancer, and diabetic patients were the 34 subjects with gastric cancer plus diabetes. Liver biopsy was taken from the curative surgery. The human study was conducted based on the guidelines laid down in the declaration of Helsinki. The informed consents were signed by participants and the experimental protocol was approved by the clinical research ethics committee of Anhui Medical University.

Animal grouping

Five-week-old male C57BL/6J and KKA^y (KK.Cg-Ay/J) mice were from Beijing Vital River. The housing unit was maintained at constant temperature 22–25 °C and 50%–60% relative humidity with a 12/12-hour light/dark cycle and free access to tap water. KKA^y mice were fed with commercial high-fat diet (BEIJING HFK Bio-Technology Co., Ltd., Beijing, China) ad libitum for 4 weeks to increase their plasma glucose levels. After 4 weeks, all mice were divided into 4 groups (10-12 mice per group), including C57BL/6J fed with standard diet (SD, LAD3001G, Trophic Animal Feed High-Tech Co., Ltd, China) (C57BL/6J-SD) and ketogenic diet (KD, TP 201455, Trophic Animal Feed High-Tech Co., Ltd, China) (C57BL/6J-KD), and KKA^y fed with SD (KKA^y-SD) and KD (KKA^y-KD). The composition of the diet was listed in Table S1 (Additional file 1). All mice were fed for 16 weeks. The food and water intakes were measured three times a week and taken by the average. Body weight and fasting plasma glucose (fasted for 6-8 hours) were recorded once a week. Feeding efficiency was calculated as body weight gain (mg) per kcal food consumed. Our procedures on mice obeyed the guidelines for humane treatment set by the Association of Laboratory Animal Sciences at Anhui Medical University.

GTT and ITT tests

Fasting glucose was measured weekly by Roche blood glucose meter. Glucose tolerance test (GTT) and insulin tolerance test (ITT) were performed before mice were sacrificed, the intraperitoneal injection concentrations of glucose and insulin were 2 mg/g body weight and 0.7 mU/g body weight, respectively. Blood glucose samples were tested at 0, 30, 60, 90, 120, 150 min and 0, 20, 40, 60, 80, 100, 120 min, respectively. Area-under-curve (AUC) was calculated by the trapezoid rule.

Murine tissue and blood sample collection

By the end of experiment, after 8 h fasting, all mice were euthanized with 10% chloral hydrate and then killed by cervical dislocation to obtain tissues and blood samples. Blood was immediately centrifuged at 3000 rpm for 10 minutes and the levels of insulin in plasma were detected by enzyme linked immunosorbent assay (ELISA) kits. The homeostatic model assessment of insulin resistance (HOMA-IR) index was calculated using the following formula: fasting insulin levels (mIU/L) × fasting glucose levels (mmol/L)/22.5. The remaining plasma was stored at -80°C for later analysis. The liver tissues were rinsed with cold phosphate-buffered saline (PBS). Small portions of liver tissues were fixed in 4% paraformaldehyde solution for oil red O and hematoxylin-eosin staining respectively. Then two-third of liver per mice was frozen in liquid nitrogen immediately and kept at -80 °C for immunoblotting and biochemical analysis. The remaining livers were preserved in RNAlater for qRT-PCR test. TC, TG, ALT and AST were determined using enzymatic kits in accordance with the manufacturer's instruction.

Cell culture

McArdle 7777 rat hepatoma cells were obtained from the American Type Culture Collection (Manassas, VA, USA, cat# CRL-1601). McArdle 7777 cells were cultured in DMEM with high glucose concentration (25 mmol/L), supplemented with 10 % FBS and 1 % penicillin/streptomycin in an incubation chamber with 5% CO_2 at 37℃. The concentration and time of β-hydroxybutyric acid (β-HB) treatment were selected depended on cell counting kit-8 (CCK-8) test. Specifically, McArdle liver cells were seeded in the 96-well plates for 24 h. Then by the β-HB treatment with a series of concentrations (0, 0.25, 1, 2, 4, mM) and times (0, 12, 24, 48 h), CCK-8 reagents (10ul) were added into the treated cells. Next, the cells were incubated for 1-4 h at 37 °C. Simultaneously, the medium was treated in the same way. The absorbance at 450 nm was detected by the microplate reader. Cellular viability was calculated by the absorbance values, by which the most suitable treatment concentration and time were determined.

Quantitative real-time PCR

The total RNAs were extracted using RNAex Pro reagent. The genomic DNA was removed using RNase-free DNase. Purified total RNA (1μg) was reverse-transcribed using reverse transcriptase. qRT-PCR was performed with a Roche Light Cycler 480 System with SYBR Green Super Mix using gene-specific primers (Additional file 1: Table S2). The comparative Ct method was used to determine the amount of target, normalized to an endogenous reference (β-Actin) and relative to a calibrator ($2^{-\triangle\triangle Ct}$).

Immunoblotting

McArdle 7777 cells and liver tissues (30 mg/per sample) were homogenized in lysis buffer, respectively. Total lysates (20μg per well) were separated electrophoretically by 10% SDS-PAGE and transferred onto PVDF membranes. The membranes were respectively incubated for 24 h with CHOP, PES1, p300, SREBP1c, SREBP2, FASN, SCD1, NLRP3, Caspase 1, GSDMD antibodies at 4℃. β-Actin was used as a loading control. After being washed 8 min for 4 times with TBST buffer, the membranes were incubated with secondary antibodies for 60 min. The enhanced chemiluminescence reagent was used. The signal was then detected by the digital imaging equipment.

Immunofluorescence

McArdle 7777 cells were seeded onto 12-well plate containing cell climbing slides for 24 h. After β-HB treatments, cells were washed thrice with PBS and fixed with 4% paraformaldehyde for 20 min. Nonspecific binding sites were blocked with 5% normal bovine serum in PBS. The 12-well plates were incubated with the mixture of primary antibodies including PES1 (1:250) and SREBP1c (1:250) at 4°C overnight. After PBS washing, the 12-well plates were incubated for 60 min with the Alexa Fluor 488 conjugated secondary antibody (ab150077, Abcam) or Alexa Fluor 568 conjugated secondary antibody (ab175473, Abcam). Cell climbing slides were taken out from the 12-well plate and buckled upside down on the glass slide containing DAPI. All sections were mounted and observed by a confocal microscope (LSM880, Zeiss).

RNA interference of Pes1 and caspase1

Rat *Pes1* and *caspase1* small interfering RNA (siRNA) and Lipofectamine 3000 (L3000008, Invitrogen Life Technologies Crop) were mixed in serum-free medium for 20 min, respectively. Then the mixture was added to the culture medium to transfect McArdle 7777 cells. After 6 h, the cells continue to be cultured in fresh medium for 48 h. Finally, cells were collected for subsequent measuring TG, TC, and running Western Blotting and qRT-PCR. The sequences of *Pes1* siRNA were 5'-UGAAGAAGCGAGAGAAGUATTT-3' (forward) and 5'- UACUUCUCUCGC UUCUUCATT-3' (reverse). The sequences of *caspase1* siRNA were 5'-AGGAAGA GAUGGAUACAAUTT-3' (forward) and 5'-AUUGUAUCCAUCUCUCUUCCUTT- 3' (reverse). The scrambled siRNA control sequences were 5'-UUCUCCGAA CGUGUCACGUTT-3' (forward) and 5'-ACGUGACACGUUCGGAGAATT-3' (reverse).

Overexpression of Pes1 in vitro

The purified plasmid of *Pes1*-flag, P3000 and Lipofectamine 3000 were mixed in serum-free medium for 20 min. Then the mixture was added into the culture medium to transfect McArdle 7777 cells for 6 h. After being cultured in fresh medium for 24 h, the cells were divided into 3 groups for different treatments, including negative control (without transfection of *Pes1* plasmid or any reagent), *Pes1*-plasmid and *Pes1*-plasmid plus β-HB. Being cultured for 24 h, cells were collected for subsequent assays of TG, TC, Western Blotting and qRT-PCR.

Chromatin immunoprecipitation

The binding of CHOP (C/EBP-homologous protein) to the *Pes1* promoter, PES1 binding to the *p300* and *caspase1* promoters were analyzed by chromatin immunoprecipitation (ChIP). Briefly, cells were crosslinked with 1% formaldehyde for 10 min, neutralized with 125 mM glycine pH 2.5 and washed in PBS. Nuclei were prepared by hypotonic lysis (5mM Pipes pH 6.8, 85 mM KCl, 0.5% NP40) and centrifugation, and resuspended in SDS Lysis Buffer, and incubated on ice for 10 minutes to be fully lysed. Chromatin was sonicated with bioruptor (Diagenode) to be 200-1000 bp average fragment size and cleared by centrifugation. The anti-CHOP, anti-PES1 antibodies or control rabbit IgG (AC005, ABclonal

Technology Co.,Ltd) was respectively added into an aliquot of 200 μl sonicated lysate, and then 20 μl washed protein A/G-agarose beads (sc-2003, Santa Cruz Biotechnology) was added. The mixture was rotated at 4 C° for 2 h, and then centrifuged at 1000g for 1min at 4 C° to wash the beads. The washed beads were resuspended in TE buffer, vortexed 10 s and boiled for 10 min. The samples and sonicated lysates were treated with 1μl of 20mg/ml proteinase K. After being centrifuged at 12,000g for 5 min at 4 C°, the digested DNA was used for qRT-PCR assay. Primers for the CHOP binding site in *Pes1* promoter, the PES1 binding site in the rat *p300* and *caspase1* promoters were as follows: CHOP-*Pes1* binding site (forward) 5’- CTGGTACGTGGGTGCAGTTTGG -3’, CHOP-*Pes1* binding site (reverse) 5’-CACACAGGGATGAACATAAGTGAGA GG-3’; PES1-*p300* binding site (forward) 5'-TCCTCTTGCTGTCTGACTTGTTTGA G-3', PES1-*p300* binding site (reverse) 5'-AAGATGTTGAGCCTGTTCTCTGAGTT C-3'; PES1-*caspase*1 binding site (forward) 5'-GGAGCAGGGAAACGATGTATGT GAG-3', PES1-*caspase*1 binding site (reverse) 5'-TTGCCCTCAGGATCTTGTCTG TTTAAG-3'.

Co-immunoprecipitation

The every extracted protein stock solutions from cultured cells or liver tissues were divided into 2 aliquots. The small part was directly used for input assay, and the remaining big portion was pre-cleared with protein A/G-agarose (sc-2003, Santa Cruz Biotechnology) for 2 h. The supernatant after pre-clearance was collected by centrifugation, and further divided into two equal portions. Ac-SREBP1c (Acetylated SREBP-1c), p300 and nonimmune IgG (Santa Cruz, sc-2025) antibodies were respectively added in the supernatant (2μg /per portion) and incubated at 4 °C overnight in rotating equipment. After centrifugation, the precipitates were collected and washed with cold lysis buffer for six times. The mixture of precipitates and loading buffer was boiled and then Ac-SREBP1c, p300, SREBP1c levels were detected using immunoblotting.

Liver-conditional knockout (CKO) Pes1 gene in mice

The parent of *Pes1* CKO mice were generated by collaboration with Nanjing Institute of Biomedicine, Nanjing University (Jiangsu, China). Positive F1 generation mice were achieved by CRISPR-cas9 technology. And hepatic *Pes1* CKO mice were obtained by positive F1 generation crossing with ALB-Cre mice. Genotyping was performed by PCR using genomic DNA extracted from mouse tails at 3-4 weeks. The mice were classified into wild-type littermates (fl/fl, wt/wt) and *Pes1* $^{(-/-)}$ (fl/fl, mut/wt) relied on genotype. The primer sequences for the transgenic Cre mice were as follows: Cre sense, 5’-TTGGCCCCTTACCATAACTG-3’; Cre antisense, 5’-GAAGCAGAAG CTTAGGAAGATGG-3’. The primer sequences for genotyping the *Pes1* alleles were as follows: shared sense, 5’-TTCCTCACCCTCAGCATTAG’; wild-type antisense, 5’-GAGATAGACTGCAAGGCACTGT-3’. Only male mice were used for all analyses (10-15 mice per group). After 16 weeks, mice were sacrificed after anesthetization to obtain the serum and livers for consecutive measuring TG, TC, and running Western Blotting and qRT-PCR.

Statistical analysis

Normally distributed data were expressed as mean ± SEMs. The continuous variables were analyzed either by Student's t test, or by ANOVA followed by Student-Newman-Keuls q test for multiple comparisons. χ^2 test was used to examine differences for categorical variables. Pearson correlation analysis was used to assess the relation between hepatic *PES1* mRNA levels and plasma lipid profiles. $P < 0.05$ was considered statistically significant. The data were analyzed using SPSS version 22.0 (IBM Corporation, Armonk, USA). Graphics were constructed using GraphPad Prism 7 (GraphPad Software, San Diego, CA).

Results

T2DM substantially enhances PES1 expression in liver, which is correlated with abnormal levels of plasma triglycerides

The socio-demographic and metabolic characteristics are included in Table 1. Significant differences between controls and T2DM patients are observed in levels of FPG (t=31.834, P<0.001), HbA1c (t=20.081, P<0.001) and TG (t=4.443, P=0.043). And T2DM dramatically enhances the PES1 protein synthesis in livers of patients (Fig. 1A-1B). Meanwhile, our data showed that T2DM significantly increases *PES1* mRNA levels as well (Fig. 1C). To explore the possible relationship of hepatic *PES1* mRNA levels and plasma lipid concentrations, the statistical correlations between controls and diabetic patients were evaluated. A plot of plasma triglyceride concentrations versus hepatic *PES1* mRNA levels showed significant positive segregation of controls and T2DM patients (r=0.6099, P=0.0004) (Fig. 1D). However, the plots of plasma TC, HDL-C and LDL-C levels versus hepatic *PES1* mRNA levels showed no significant disparity (all P>0.05, Fig. 1E-1G).

Long-term KD intervention improved the hyperglycemia and insulin resistance in diabetic mice

After 16 weeks of KD intervention, body weights in KKA^y-KD group showed no significant difference from those in the KKA^y-SD groups, the similar results were also observed in the C57BL6J-KD group (Fig. 2A). With regard to both normal and diabetic mice, intakes of SD were significantly higher than those of KD (Fig. 2B), parallel to the consumptions of water (Fig. 2C). In terms of daily energy intake and feeding efficiency, the values by the KD and SD feeding in normal and diabetic mice were not drastically different (Fig. 2D-2E). However, the fasting plasma glucose levels were remarkably reduced in diabetic mice by KD intervention, compared to those by SD (Fig. 2F).

The ITT and GTT assays exhibited that KD could significantly ameliorate glucose tolerance and insulin sensitivity in diabetic mice (Fig. 2G-2H). Moreover, serum insulin levels and HOMA-IR in diabetic mice were obviously improved by KD treatments (Fig. 2J-2K), but no statistic difference between C57BL/6J-SD and C57BL/6J-KD. In addition, the serum β-HB levels were sharply elevated by KD feeding in both healthy and diabetic mice (Fig. 2I).

KD suppressed PES1 and improved lipid dysregulation under diabetic state

After 16 weeks of KD feeding, the current results displayed that the protein levels of CHOP, PES1, p300, SREBP1c, N'-SREBP1c, FASN and SCD1 were dramatically inhibited in both healthy and diabetic mice (Fig. 3A-3B). Histological analysis (H&E and Oil Red O staining) revealed much less pathogenesis and lipid accumulation in livers of KKA^y mice fed by KD than those by SD (Fig. 3C). Additionally, KD extraordinarily decreased plasma and hepatic TG levels in C57BL/6J and KKA^y mice, compared to SD (Fig. 3D-3E). Lastly, KD feeding in normal and diabetic mice was associated with reductions of plasma AST and ALT (Fig. 3F).

β-HB decreased PES1 and triglycerides in liver cells

β-HB, the main component of ketone bodies, was used to test the KD effect on liver cells *in vitro*. The optimized concentration and time of β-HB treatment were selected by cell viability test (Fig. S1A). The protein levels of PES1 by the β-HB treatments with different concentrations and times were dramatically lower than those by control treatment (Fig. S1B-1C). Considering the ketogenesis by the KD feeding in mice, the concentration (1 mM) of β-HB and its treatment time (24 h) were identified. The protein levels CHOP, PES1, p300, SREBP1c, N'-SREBP1c, FASN and SCD1 were greatly attenuated by the β-HB treatment *in vitro* (Fig. 4A-4B). ChIP test indicated that β-HB decreased CHOP binding to *Pes1* promoter (Fig. 4C). Consistent with the above data, the immunofluorescence showed that β-HB suppressed PES1 and SREBP1c proteins in nucleus of McArdle cells (Fig. 4D). Moreover, medium and cellular TG levels were markedly declined by β-HB treatment (Fig. 4E-4F).

In vitro knockdown of Pes1 impaired medium and cellular triglyceride production in liver cells.

To probe PES1 modulating role, the siRNA knockdown of *Pes1* was performed in McArdle cells. The levels of PES1 protein were significantly downregulated in the treated cells (Fig. 5A-5B). Simultaneously, the medium and cellular triglycerides, and the levels of p300, SREBP1c, N'-SREBP1c, FASN and SCD1 in the treated cells were dramatically reduced compared to those in control cells (Fig. 5A-5D).

In vitro supplementation of Pes1 promoted cellular triglyceride levels, but β-HB treatment eliminated the elevation

The overexpression of *Pes1 in vitro* was performed to further confirm the key role of PES1 in lipid metabolism. The current results showed that the protein levels of p300, SREBP1c, N'-SREBP1c, FASN and SCD1 were significantly increased by *Pes1* overexpression, but the effects were sharply reversed by β-HB treatment (Fig. 5E-5F). Furthermore, overexpression of *Pes1* significantly increased medium and cellular triglycerides, while β-HB treatment eliminated those increases (Fig. 5G-5H).

Liver-specific Pes1 knockout in mice decreased the lipid generation

The exon 2 in murine *Pes1* gene was targeted by CRISPR-Cas9/RNA system gene targeting technology (Fig. 6A). The liver mRNA levels of *Pes1* were almost completely eliminated in CKO mice by qRT-PCR test (Fig. S2). After 16 weeks of feeding, no significant difference of body weights between wild-type

littermates (fl/fl, wt/wt) and *Pes1*-CKO mice (fl/fl, mut/wt) was found (Fig. 6B). But the protein levels of p300, SREBP1c, N'-SREBP1c, FASN and SCD1 were dramatically downregulated in *Pes1*-CKO mice (Fig. 6C-6D). Moreover, the weights of liver and subcutaneous fat, and the ratios of liver/body weight, fat/body weight were also substantially declined in *Pes1*-CKO mice (Fig. 6E-6G). Likewise, plasma and hepatic triglycerides, plasma AST and ALT in *Pe*s1-CKO mice were sharply lower than those in the wild-type littermates (Fig. 6H-6J).

β-HB lowered PES1 binding to the p300 promoter and downregulated PES1 mediated acetylation of SREBP1c

The ChIP experiment revealed that β-HB reduced PES1 binding to the *p300* promoter, resulting in downregulation of *p300* gene expression (Fig. 7A). To determine whether β-HB affects PES1 regulated SREBP1c activity, acetylation assays *in vitro* and *in vivo* were performed. Additionally, co-IP was used to explore the interaction between p300 and SREBP1c. We found that *Pes1* silence in hepatocytes reduced the interaction between p300 and SREBP1c (Fig. 7B). Contrastingly, *Pes1* overexpression increased the interaction, which was however impaired under β-HB treatment (Fig. 7C). Subsequently, β-HB treatment by hepatocytes inhibited the acetylation of SREBP1c (Fig. 7D). Next, whether the acetylation of SREBP1c is regulated by PES1 *in vivo* was also investigated. Our current data indicated that *Pes1* knockout in mice significantly reduced the interaction between p300 and SREBP1c (Fig. 7E). And KD feeding in normal and diabetic mice showed that the acetylation of SREBP1c was sharply suppressed (Fig. 7F).

KD and β-HB decreased inflammation responses by downregulating PES1

According to the published reports, inflammation might promote lipogenesis (Todoric et al. 2020). In the present study, the levels of Recombinant NLR Family Pyrin Domain Containing Protein 3 (NLRP3), caspase1, cleaved-caspase1, gasdermin-D (GSDMD), and cleaved-GSDMD were found to be significantly inhibited in normal and diabetic mice fed with KD, compared to those with SD (Fig. 8A-8B). Simultaneously, KD led to much less inflammation responses in mice than SD, as indicated by decreased pro-inflammatory factor levels (*IL-1β* and *IL-18*) in the murine livers (Fig. 8C), similar to the results of β-HB treated hepatocytes (Fig. 8D-8F). Furthermore, the silence or supplementation of *Pes1 in vitro* elicited the suppression or enhancement of NLRP3, caspase 1, cleaved-caspase 1, GSDMD, cleaved-GSDMD, *IL-1β* and *IL-18* levels, respectively (Fig. 8G-8I). More interestingly, the enhancement by overexpression of *Pes1* was also impairedwithβ-HB treatment *in vitro* (Fig. 8J-8I). In addition, consistent with *Pes1* silence *in vitro*, the similar results were observed in *Pes1* knockout mice (Fig. 8M-8O).

β-HB decreased PES1 binding to the caspase1 promoter and knockdown of caspase1 reduced medium and cellular triglycerides in liver cells

To verify caspase1 modulating role, the siRNA knockdown of *caspase1* was carried out in hepatocytes. The knockdown results suggested that the levels of caspase1 and GSDMD were declined (Fig. 9A-9B), and that the mRNA levels of *IL-1β* and *IL-18* were suppressed as well (Fig. 9C). Furthermore, medium and cellular TG levels were dramatically inhibited in *caspase1* siRNA treated cells (Fig. 9D-9E).

Mechanistically, β-HB treatment in liver cells lowered PES1 binding to *caspase1* gene promoter, resulting in the downregulation of *caspase1* gene expression (Fig. 9F). The schematic diagram of entire study is presented in the Figure 9G.

Discussion

Recently, clinical studies indicated that KD was effective in improving metabolic parameters of weight, glycemia, and lipid profiles in patients with overweight or obesity, especially in those with preexisting diabetes (Choi et al. 2020; Li et al. 2020). In our current study, although the high glucose level is naturally dropped in KK*A*^{y} murine model after age of 18 weeks according to the literature (Zhang et al. 2020), we still observed the effects of KD on lowering plasma glucose and improving insulin sensitivity in T2DM mice compared to those of SD, which was consistent with previous publication (Yang et al. 2021). In addition, Guo YZ et al also reported that the plasma and hepatic TG levels were evidently dropped in normal and T2DM mice fed by KD (Guo et al. 2020), which are exact resemblance to our current study.

β-HB, as the predominant component of ketone body, has been demonstrated to serve as molecular scaffold that regulates cellular function by directly activating hydroxy-carboxylic acid receptors, and to be involved in multiple physiological processes including metabolism and inflammation (Offermanns et al. 2017). Furthermore, compelling evidence based on animal study suggested that KD may block NLRP3 inflammasome-mediated IL-1β and IL-18 production (Youm et al. 2015), which is in concordance with our current observation. In this study, the levels of β-HB in normal mice were higher than those in diabetic mice. This is because FGF21 levels are usually upregulated in response to ketogenesis, but FGF 21 levels are impeded in KK*A*^{y} mice with KD intervention (Li et al. 2018; Handa et al. 2014). Consequently, the ketogenesis by KD was mitigated in KK*A*^{y} mice, nevertheless the ketone level was still legitimate for current study based on the preceding finding (Yotsumoto et al. 2005).Furthermore, emerging evidence from long-term KD intervention in T2DM patients supports that the ketogenesis was also attenuated (Casanueva et al. 2020). In addition, the experiment from β-HB injection in animal showed that lipid peroxides were decreased by half levels in kidney (Shimazu et al. 2013). In keeping with observation, additional proof from cell study suggested that anti-lipid peroxidation effect of β-HB could exert a protection role in microglial apoptosis (Sabokdast et al. 2015).

Of note, we discerned that PES1 levels were downregulated by KD feeding in normal and diabetic mice and by β-HB treatment in cells. Previous finding indicated that circANRIL could play an important role in atheroprotection by inhibiting PES1 (Holdt et al. 2016), which is in line with our current study. Although there is no report about the association between PES1 and inflammation, PES1 was overtly upregulated in various malignant tumors that were positively correlated with inflammation factors (Karki et al. 2017). And inflammation was found to be associated with nonalcoholic steatohepatitis (Kazankov et al. 2019).

Moreover, our current study unveiled that β-HB may reduce CHOP binding to *Pes1* promoter, resulting in the downregulation of PES1. The decreased PES1 protein level impaired its binding to *p300* and *caspase1* promoters, causing the declined expressions of p300 and caspase1, thus undermining p300

mediated acetylation of SREBP1c and inflammation response. CHOP, a key apoptosis-promoting factor, tightly controls the gene transcription and has pivotal roles in lipid accumulation, adipogenesis and inflammatory action (Liu et al. 2018; Maris et al. 2012; Allagnat et al. 2012). And one report has showed that KD intervention in mice could reduce the expression of CHOP (Yu et al. 2020), which is consistent to our current study. In addition, it has also been proposed that SREBP-1c binds to its lipogenic target genes, such as fatty acid synthase (FASN) and stearoyl-CoA desaturase 1 (SCD1), thereby stimulating *de novo* lipogenesis (Li et al. 2015). A crucial role of SREBP-1c has been shown *in vivo* by hepatic overexpression of SREBP-1c in transgenic mice that led to increased hepatic lipid accumulation (Wang et al. 2015). Accumulating evidence showed that the acetylation of SREBP1c increased its stability and activity, and SREBP-1c is acetylated by p300 at Lys-289 and Lys-309 (Ponugoti et al. 2010). In this report, after *Pes1* gene was knocked down, the interaction between SREBP1c and p300 was significantly inhibited, consistent with the observation in *Pes1*-CKO mice. Moreover, the interaction between SREBP1c and p300 was obviously strengthened during *Pes1* gene overexpression, which was however impeded by β-HB treatment. Furthermore, our current study also suggested that β-HB and KD remarkably reduced the SREBP1c activity *via* inhibiting the acetylation of SREBP1c. Additionally, caspase1 and NLRP3, as regulatory molecules of lipid metabolism, were reported to promote the release of mature IL-1β and to interfere insulin signaling and production, subsequently leading to the lipogenesis and fat accumulation (Anand et al. 2020). Based on *caspase1* knockdown in hepatocytes, our current data showed that medium and cellular TG levels were clearly curbed, which is similar to the protection role in *caspase1* knockout mice fed with high fat diet (Stienstra et al. 2011). Collectively, these results suggest that β-HB treatment in cells and KD feeding in mice greatly reduced lipid production or accumulation *via* downregulating PES1 mediated acetylation of SREBP1c and inflammation pathways.

The current study explored a novel mechanism of KD intervention in diabetic mice, which may have translational potential and clinical implications by finding a PES1 inhibitor. However, the interpretation of this study so far is still limited due to the lack of human intervention data, and PES1 function and its mediated mechanism by KD intervention in human is needed in future. In addition, the metabolic factors regulating PES1 expression under T2DM condition are not elucidated yet.

Conclusion

In summary, our current findings demonstrate that KD may ameliorate lipid deposition in type 2 diabetic mice by downregulating PES1 mediated acetylation of SREBP1c and inflammation pathways. This study may provide a novel insight to help understand the mechanisms underlying T2DM related lipid dysregulation and may contribute a new pharmaceutical target for T2DM treatment.

Abbreviations

ALT: alanine aminotransferase; AST: aspartate aminotransferase; AUC: area-under curve; CCK-8: cell counting kit-8; CHOP: C/EBP-homologous protein; CKO: conditional knockout; ELISA: enzyme linked immunosorbent assay; FASN: fatty acid synthase; GTT: glucose tolerance test; GSDMD: Gasdermin D;

HOMA-IR: homeostatic model assessment of insulin resistance; IR: insulin resistance; ITT: insulin tolerance test; KD: ketogenic diet; NLRP3: Recombinant NLR Family Pyrin Domain Containing Protein 3; PBS: phosphate-buffered saline; PES1: pescadillo 1; qRT-PCR: quantitative real-time PCR; SD: standard diet; siRNA: small interfering RNA; SREBP1c: sterol regulatory element binding protein 1c; SREBP2: sterol regulatory element binding protein 2; T2DM: type 2 diabetes mellitus; TC: total cholesterol; TG: triglycerides; β-HB: β-hydroxybutyric acid

Declarations

Acknowledgements

We would like to thank all the colleagues in our research team.

Author's contribution

K.C and Z.J designed the research, provide financial support and revised/edited the manuscript; Y.L provided partial research fund; J.Z, J.L, and Y.J performed all experiments; J.Z collected and analyzed the data; J.Z and Y. L wrote the draft of manuscript. All authors discussed and approved the manuscript.

Funding: This work is supported by the National Natural Science Foundation of China (NSFC, 81570786 to K.C, 82070986 to Z.J, 81770295 to Y.L), Wanjiang scholar grants from Anhui Province of China (9101041203 to Z.J), Outstanding young scientist program of Anhui Province (2008085J34 to Y.L)

Ethics approval and consent to participate

The study was approved by the Institutional Animal Care and Use Committee of Anhui Medical University and performed following the relevant guidelines and regulations.

Consent for publication

Not applicable.

Competing interests

The authors declare no conflict of interest.

Supplementary Information

The online version contains supplementary material.

Author details

[1]Department of Nutrition and Food Hygiene, Anhui Medical University School of Public Health, Hefei, Anhui 230032,China. [2]Department of Anesthesiology, the First Affiliated Hospital, Anhui Medical

University, Hefei, Anhui 230032, China. [3]Department of Health Inspection and Quarantine, Anhui Medical University School of Public Health, Hefei, Anhui 230032, China. [4]Department of Ophthalmology, the Second Affiliated Hospital, Anhui Medical University, Hefei, Anhui 230021, China.

References

1. Abbasi J. Interest in the ketogenic diet grows for weight loss and type 2 diabetes. JAMA. 2018;319:215-217.
2. Allagnat F, Fukaya M, Nogueira TC, Delaroche D, Welsh N, Marselli L, et al. C/EBP homologous protein contributes to cytokine-induced pro-inflammatory responses and apoptosis in β-cells. Cell Death Differ. 2012;19:1836-46.
3. Allende ML, Amsterdam A, Becker T, Kawakami K, Gaiano N, Hopkins N. Insertional mutagenesis in zebrafish identifies two novel genes, pescadillo and dead eye, essential for embryonic development. Genes Dev. 1996;10:3141-3155.
4. Allen BG, Bhatia SK, Anderson CM, Eichenberger-Gilmore JM, Sibenaller ZA, Mapuskar KA, et al. Ketogenic diets as an adjuvant cancer therapy: history and potential mechanism. Redox Biol. 2014;2:963-70.
5. Anand PK. Lipids, inflammasomes, metabolism, and disease. Immunol Rev. 2020;297:108-122.
6. Augustin K, Khabbush A, Williams S, Eaton S, Orford M, Cross JH, et al. Mechanisms of action for the medium-chain triglyceride ketogenic diet in neurological and metabolic disorders. Lancet Neurol 2018;17:84-93.
7. Casanueva FF, Castellana M, Bellido D, Trimboli P, Castro AI, Sajoux I, et al. Ketogenic diets as treatment of obesity and type 2 diabetes mellitus. Rev Endocr Metab Disord. 2020;21:381-397.
8. Castellana M, Conte E, Cignarelli A, Perrini S, Giustina A, Giovanella L, et al. Efficacy and safety of very low calorie ketogenic diet (VLCKD) in patients with overweight and obesity: A systematic review and meta-analysis.Rev Endocr Metab Disord. 2020;21:5-16.
9. Cheng L, Li J, Han Y, Lin J, Niu C, Zhou Z, et al. PES1 promotes breast cancer by differentially regulating ERα and ERβ. J Clin Invest. 2012;122:2857-70.
10. Cheng L, Yuan B, Ying S, Niu C, Mai H, Guan X, et al. PES1 is a critical component of telomerase assembly and regulates cellular senescence. Sci Adv. 2019;5:eaav1090.
11. Choi YJ, Jeon SM, Shin S. Impact of a ketogenic diet on metabolic parameters in patients with obesity or overweight and with or without type 2 diabetes: A meta-analysis of randomized controlled trials. Nutrients. 2020;12:2005.
12. Du YC, Stillman B. Yph1p, an ORC-interacting protein: potential links between cell proliferation control, DNA replication, and ribosome biogenesis. Cell. 2002;109:835-848.
13. Ellenbroek JH, van Dijck L, Töns HA, Rabelink TJ, Carlotti F, Ballieux BE, et al. Long-term ketogenic diet causes glucose intolerance and reduced β- and α-cell mass but no weight loss in mice. Am J Physiol Endocrinol Metab. 2014; 306:E552-E558.

14. Fan P, Wang B, Meng Z, Zhao J, Jin X. PES1 is transcriptionally regulated by BRD4 and promotes cell proliferation and glycolysis in hepatocellular carcinoma. Int J Biochem Cell Biol. 2018;104:1-8.
15. Gentile CL, Weir TL. The gut microbiota at the intersection of diet and human health. Science. 2018;362:776-780.
16. Guo Y, Zhang C, Shang FF, Luo M, You Y, Zhai Q, et al. Ketogenic diet ameliorates cardiac dysfunction via balancing mitochondrial dynamics and inhibiting apoptosis in type 2 diabetic mice. Aging Dis. 2020;11:229-240.
17. Handa K, Inukai K, Onuma H, Kudo A, Nakagawa F, Tsugawa K, et al. Long-term low carbohydrate diet leads to deleterious metabolic manifestations in diabetic mice. PLoS One. 2014;9:e104948.
18. Holdt LM, Stahringer A, Sass K, Pichler G, Kulak NA, Wilfert W, et al. Circular non-coding RNA ANRIL modulates ribosomal RNA maturation and atherosclerosis in humans. Nat Commun. 2016;7:12429.
19. Karki R, Man SM, Kanneganti TD. Inflammasomes and Cancer. Cancer Immunol Res. 2017;5:94-99.
20. Kazankov K, Jørgensen SMD, Thomsen KL, Møller HJ, Vilstrup H, George J, et al. The role of macrophages in nonalcoholic fatty liver disease and nonalcoholic steatohepatitis. Nat Rev Gastroenterol Hepatol. 2019;16:145-159.
21. Klil-Drori AJ, Azoulay L, Pollak MN. Cancer, obesity, diabetes, and antidiabetic drugs: is the fog clearing? Nat Rev Clin Oncol. 2017;14(2):85-99.
22. Li J, Zhuang Q, Lan X, Zeng G, Jiang X, Huang Z. PES1 differentially regulates the expression of ERα and ERβ in ovarian cancer. IUBMB Life. 2013;65:1017-25.
23. Li J, Huang Q, Long X, Zhang J, Huang X, Aa J, et al. CD147 reprograms fatty acid metabolism in hepatocellular carcinoma cells through Akt/mTOR/ SREBP1c and P38/PPARα pathways. J Hepatol. 2015;63:1378- 1389.
24. Li W, Ji M, Lin Y, Miao Y, Chen S, Li H. DEPP/DEPP1/C10ORF10 regulates hepatic glucose and fat metabolism partly via ROS-induced FGF21. FASEB J. 2018;32:5459-5469.
25. Li Z, Heber D. Ketogenic diets. JAMA. 2020;323:386.
26. Liu R, Li X, Huang Z, Zhao D, Ganesh BS, Lai G, et al. C/EBP homologous protein-induced loss of intestinal epithelial stemness contributes to bile duct ligation-induced cholestatic liver injury in mice. Hepatology. 2018;67:1441-1457.
27. Magliano DJ, Sacre JW, Harding JL, Gregg EW, Zimmet PZ, Shaw JE. Young-onset type 2 diabetes mellitus - implications for morbidity and mortality. Nat Rev Endocrinol. 2020;16:321-331.
28. Maris M, Overbergh L, Gysemans C, Waget A, Cardozo AK, Verdrengh E, et al. Deletion of C/EBP homologous protein (Chop) in C57BL/6 mice dissociates obesity from insulin resistance. Diabetologia. 2012;55:1167-78.
29. McGuire DK, Van de Werf F, Armstrong PW, Standl E, Koglin J, Green JB, et al. Association between Sitagliptin use and heart failure hospitalization and related outcomes in type 2 diabetes mellitus: secondary analysis of a randomized clinical trial. JAMA Cardiol. 2016;1:126-135.
30. Newman JC, Verdin E. β-hydroxybutyrate: A signaling metabolite. Annu Rev Nutr 2017;37:51-76.

31. Offermanns S. Hydroxy-carboxylic acid receptor actions in metabolism. Trends Endocrinol Metab. 2017;28:227-236.
32. Ponugoti B, Kim DH, Xiao Z, Smith Z, Miao J, Zang M, et al. SIRT1 deacetylates and inhibits SREBP-1C activity in regulation of hepatic lipid metabolism.J Biol Chem. 2010;285: 33959-33970.
33. Sabokdast M, Habibi-Rezaei M, Moosavi-Movahedi AA, Ferdousi M, Azimzadeh-Irani E, Poursasan N. Protection by beta-hydroxybutyric acid against insulin glycation, lipid peroxidation and microglial cell apoptosis. Daru. 2015;23:42.
34. Shlomai G, Neel B, LeRoith D, Gallagher EJ. Type 2 diabetes mellitus and cancer: the role of pharmacotherapy. J Clin Oncol. 2016;34:4261-4269.
35. Shimazu T, Hirschey MD, Newman J, He W, Shirakawa K, Le Moan N, et al. Suppression of oxidative stress by β-hydroxybutyrate, an endogenous histone deacetylase inhibitor. Science. 2013;339:211-4.
36. Stienstra R, van Diepen JA, Tack CJ, Zaki MH, van de Veerdonk FL, Perera D, et al. Inflammasome is a central player in the induction of obesity and insulin resistance. Proc Natl Acad Sci U S A. 2011;108:15324-15329.
37. Todoric J, Di Caro G, Reibe S, Henstridge DC, Green CR, Vrbanac A, et al. Fructose stimulated de novo lipogenesis is promoted by inflammation. Nature metabolism. 2020;2:1034–1045.
38. Wang Y, Viscarra J, Kim SJ, Sul HS. Transcriptional regulation of hepatic lipogenesis. Nat Rev Mol Cell Biol. 2015;16:678-689.
39. Watanabe M, Tozzi R, Risi R, Tuccinardi D, Mariani S, Basciani S, et al. Beneficial effects of the ketogenic diet on nonalcoholic fatty liver disease: A comprehensive review of the literature. Obes Rev 2020;21:e13024.
40. Xu L, Li Y, Yin L, Qi Y, Sun H, Sun P, et al. miR-125a-5p ameliorates hepatic glycolipid metabolism disorder in type 2 diabetes mellitus through targeting of STAT3. Theranostics. 2018;8:5593-5609.
41. Yang Z, Mi J, Wang Y, Xue L, Liu J, Fan M, et al. Effects of low-carbohydrate diet and ketogenic diet on glucose and lipid metabolism in type 2 diabetic mice. Nutrition. 2021;89:111230.
42. Yancy WS Jr, Mitchell NS, Westman EC. Westman ketogenic diet for obesity and diabetes.JAMA Intern Med. 2019;179:1734-1735.
43. Yotsumoto T, Naitoh T, Kanaki T, Tsuruzoe N. A retinoid X receptor antagonist, HX531, improves leptin resistance without increasing plasma leptin level in KK-Ay mice under normal dietary conditions. Metabolism. 2005;54:573-578.
44. Youm YH, Nguyen KY, Grant RW, Goldberg EL, Bodogai M, Kim D, et al. The ketone metabolite β-hydroxybutyrate blocks NLRP3 inflammasome-mediated inflammatory disease. Nat Med. 2015;21:263-9.
45. Yu Y, Wang F, Wang J, Zhang D, Zhao X. Ketogenic diet attenuates aging-associated myocardial remodeling and dysfunction in mice. Exp Gerontol. 2020;140:111058.
46. Zhang J, Zhang Y, Yang X, Wang J, Xu Y, Wang R, et al. Diabetic bladder dysfunction in T2D KK-Ay mice and its changes in the level of relevant gene expression. Biomed Pharmacother.

2020;131:110706.

47. Zhang X, Qin J, Zhao Y, Shi J, Lan R, Gan Y, et al. Long-term ketogenic diet contributes to glycemic control but promotes lipid accumulation and hepatic steatosis in type 2 diabetic mice. Nutr Res. 2016;36:349-358.
48. Zheng Y, Ley SH, Hu FB. Global aetiology and epidemiology of type 2 diabetes mellitus and its complications. Nat Rev Endocrinol. 2018;14:88-98.

Tables

Table 1 The socio-demographic and metabolic characteristics

Varibles	NC (N=32)	T2DM (N=34)	χ^2/t	P
Gender	n (%)	n (%)		
Women	22 (68.75)	20 (58.82)	0.702	0.402
Men	10 (31.25)	14 (41.18)		
Age	40.63±16.59	45.12±16.72	0.600	0.445
BMI (kg/m^2)	22.41±3.46	24.47±4.12	0.206	0.661
DBP (mmHg)	80.13±10.13	80.00±9.33	0.001	0.971
SBP (mmHg)	125.75±15.14	124.53±14.07	0.058	0.812
FPG (mmol/L)	5.09±0.58	10.72±3.95	31.834	<0.001
HbA1c (%)	4.49±0.72	8.26±2.48	20.018	<0.001
TG (mmol/L)	1.36±0.26	2.69±2.51	4.443	0.043
TC (mmol/L)	5.17±0.72	5.34±0.52	0.596	0.446
HDL-C (mmol/L)	1.32±0.23	1.25±0.24	1.051	0.299
LDL-C (mmol/L)	2.70±0.86	3.05±0.62	1.873	0.181

The total number of subjects included in the liver tissue biopsy was 66 (32 controls and 34 diabetic patients). The human participants who had some preexisting diseases or medication history, except the diabetes and newly diagnosed gastric or colorectal cancers, were excluded from the sampling. The representative tissue samples for immunoblotting and qRT-PCR were randomly selected from the total collection of 66. The immunoblots and qRT-PCR shown in Fig. 1 were the representatives of three independent experiments, respectively, for the human liver tissues. NC, normal control; T2DM, type 2 diabetes mellitus.

Figures

Fig. 1

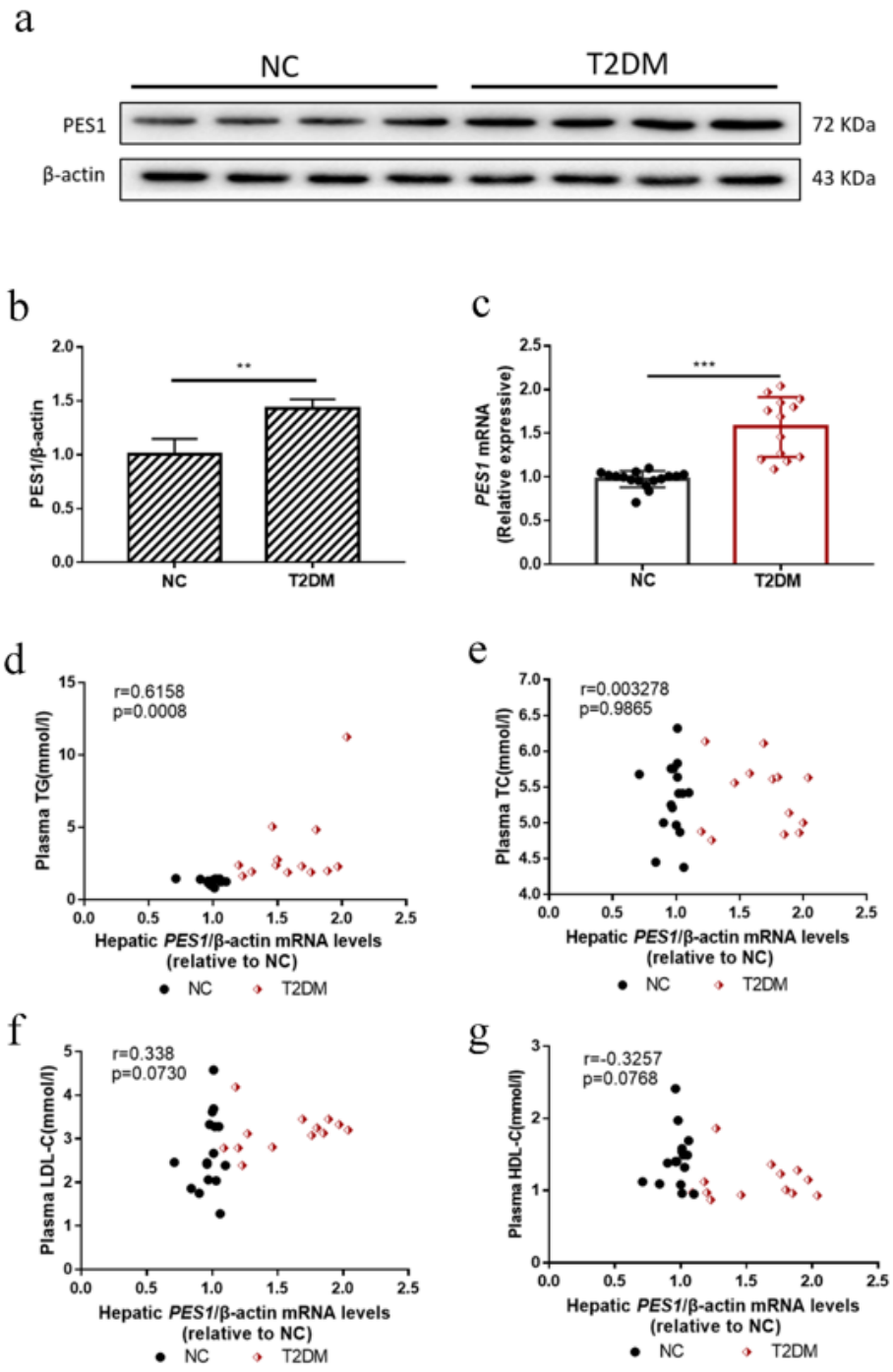

Figure 1

The elevation of PES1 expression in human diabetic livers is correlated with abnormal lipid contents. a-b Shown are the immunoblots of liver tissue homogenates both from human diabetic patients and their controls. c The mRNA expressions of PES1 were detected by quantitative RT-PCR, normalized by β-actin and expressed as 2-ΔΔCT. d-g Displayed are the plots of plasma triglyceride, total cholesterol, low density lipoprotein cholesterol and high density lipoprotein cholesterol levels versus hepatic PES1 mRNA levels

from the controls and T2DM patients. *P<0.5, **P<0.01, ***P<0.001 compare with control (Student's t-test). Each experiment was performed independently 3 times.

Fig. 2

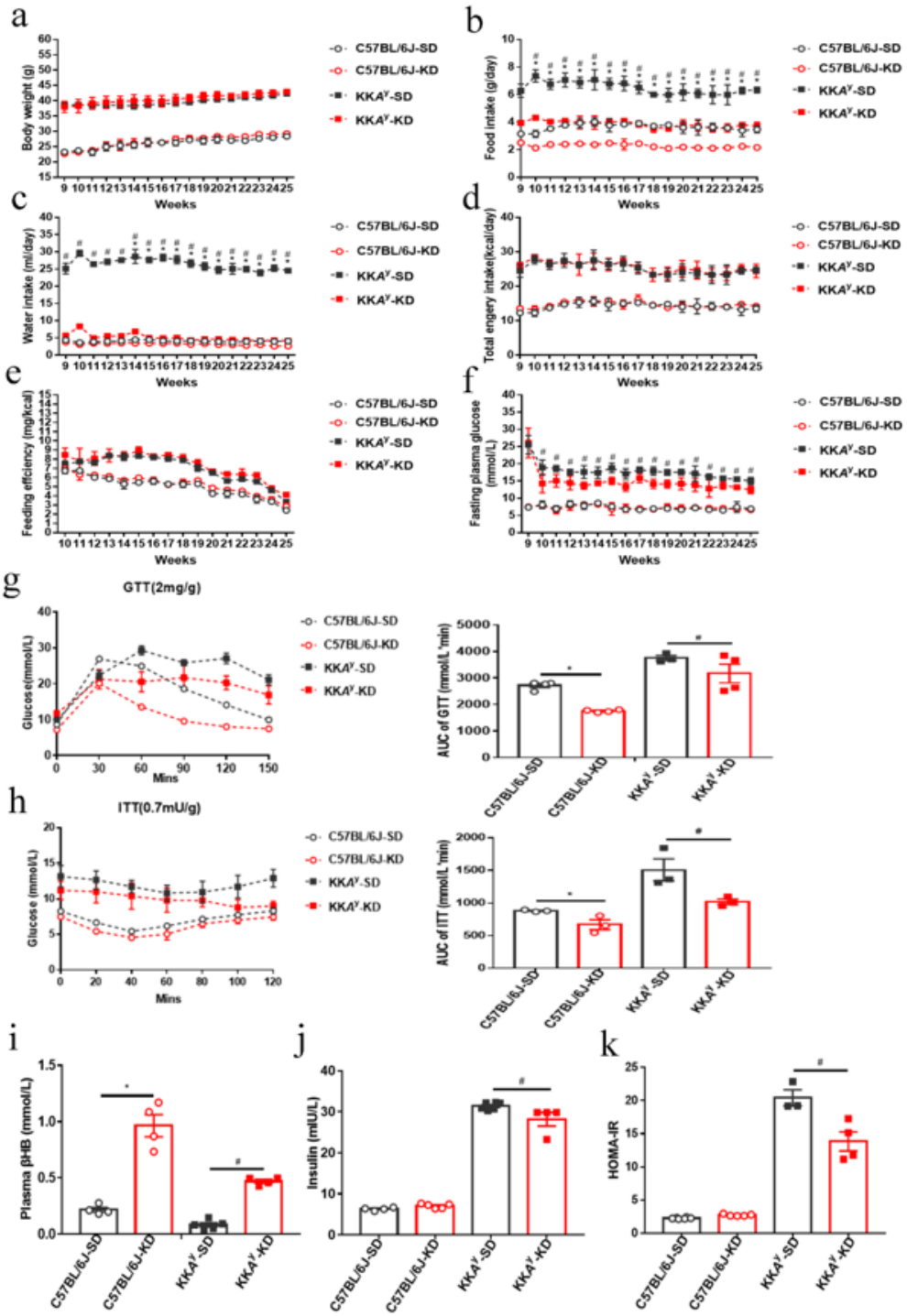

Figure 2

Ketogenic diet decreased the hyperglycemia and ameliorated insulin resistance in diabetic mice. a Shown are the changes of body weights exerted by the different food feedings in normal and diabetic mice. b Displayed are the food intakes in different groups throughout 16 weeks of feeding. c Exhibited are the

water intakes in different groups throughout 16 weeks. d Demonstrated are the total energy intakes calculated by calories in different groups throughout 16 weeks. e Unveiled are the feeding efficiencies in different groups (calculated as body weight gain (mg) per kcal food consumed). f Shown are the variations of fasting plasma glucose in different groups throughout 16 weeks. g Intraperitoneal glucose tolerance tests were performed in different groups by the end of food feeding. h Intraperitoneal insulin tolerance tests were carried out in different groups by the end of food feeding. Glucose (2 mg/g) or insulin (0.75 mU/g) was injected intraperitoneally after mice were fasted for 6-8 hours. Blood glucose samples were collected at different indicated time points and measured. Areas under the curve were calculated for the quantitative analysis. i Demonstrated are the levels of plasma β-hydroxybutyric acid (β-HB) in different groups. j Insulin levels were detected in different groups by the end of food feeding. k HOMA-IR in different groups was calculated by the formula. Data were shown as mean ± SEM for each experiment performed independently 3 times (n = 10-12 per group). SD (Standard diet), KD (Ketogenic diet). * P < 0.05 C57BL/6J-KD vs C57BL/6J-SD, # P < 0.05 KKAy-KD vs KKAy-SD (ANOVA, Student-Newman-Keuls q test).

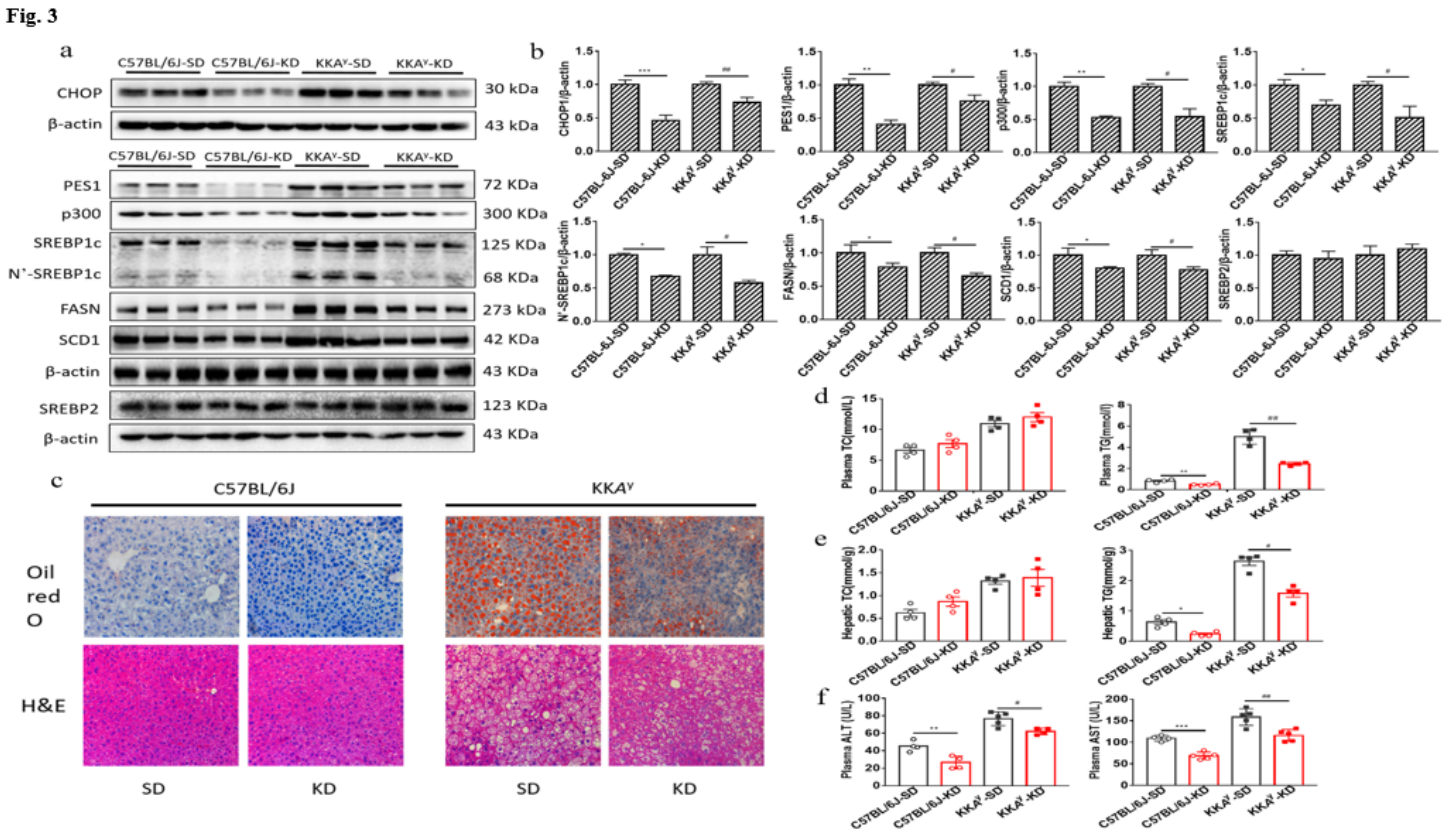

Figure 3

KD suppressed the PES1 expression and decreased plasma and hepatic TG levels in normal and diabetic mice. a-b The protein levels of hepatic CHOP, PES1, p300, SREBP1c, SREBP2, FASN and SCD1 were detected by Immunoblotting. c The oil red O and H&E staining of liver tissues were performed for different groups, original magnification, ×10. Scale bar, 50 μm. d Plasma TG and TC were assayed for different

groups by the end of food feeding. e Hepatic TG and TC levels were detected for different groups. f Plasma AST and ALT levels were measured by Reagent kit. Values are means ± SEM for each experiment performed independently 3 times. SD (Standard diet), KD (Ketogenic diet).* P < 0.05, ** P <0.01, *** P <0.001 compared with control for C57BL/6J, # P < 0.05, ## P<0.01, ### P<0.001 compared with control for KKAy (ANOVA, Student-Newman-Keuls q test).

Fig. 4

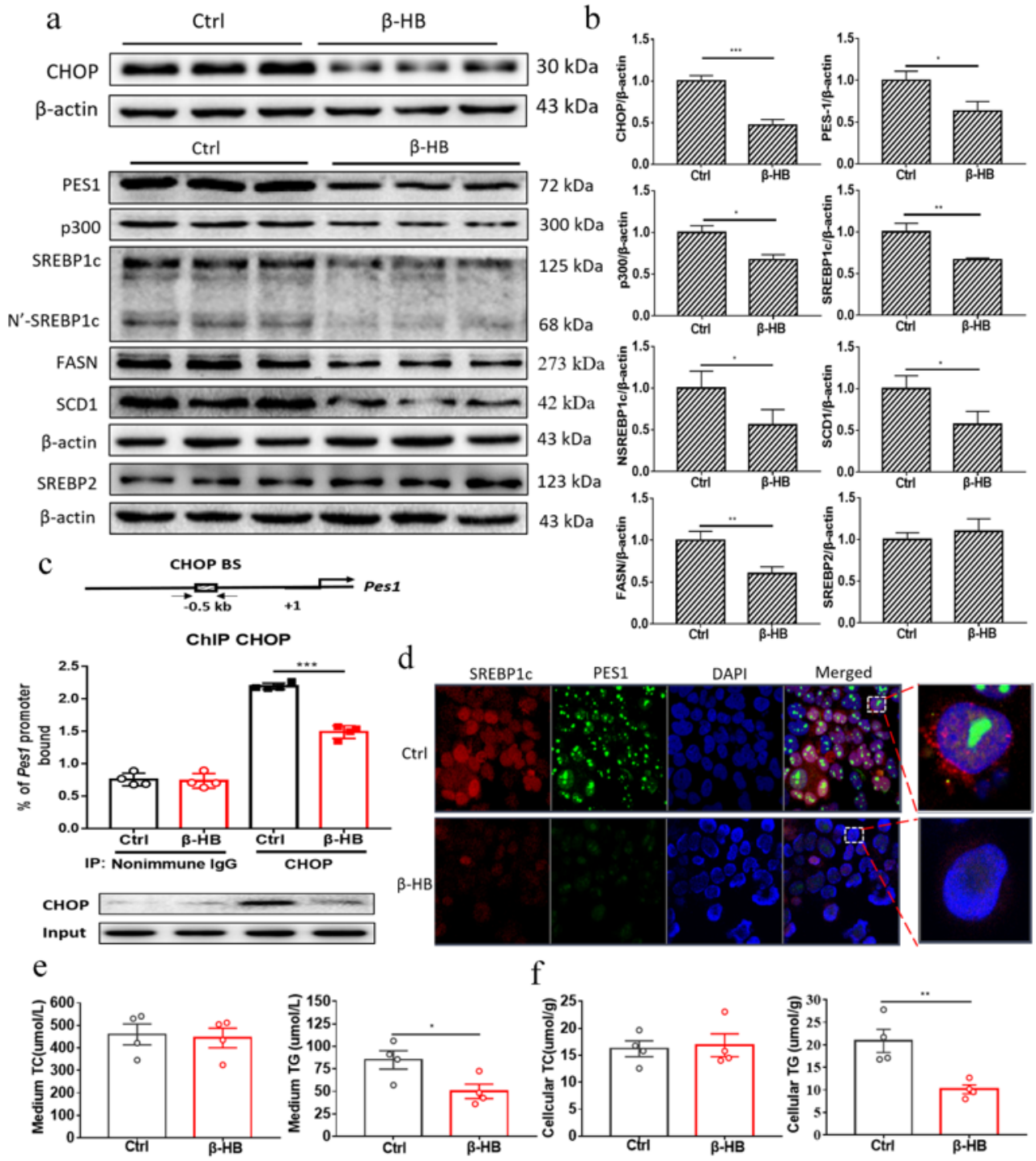

Figure 4

β-HB decreased PES1 and triglycerides in cultured liver cells. a-b The protein levels of CHOP, PES1, p300, SREBP1c, SREBP2, FASN and SCD1 in hepatocytes were detected by immunoblotting after 1 mM β-HB treatment for 24 h. c β-HB decreased CHOP binding to Pes1 promoter. d Exhibited are immunofluorescence images of β-HB-treated liver cells for PES1 and SREBP1c expressions and localization, Scale bar represents 20 um. The nuclei were stained with DAPI. e-f Demonstrated are the TG and TC levels respectively detected in the cultured media and liver cells after β-HB treatment. Ctrl (Control), β-HB (β-hydroxybutyric acid). Data were shown as mean ± SEM for each experiment performed independently 3 times. * P < 0.05, ** P < 0.01, *** P<0.001 compared with control (Student's t-test or ANOVA, Student-Newman-Keuls q test).

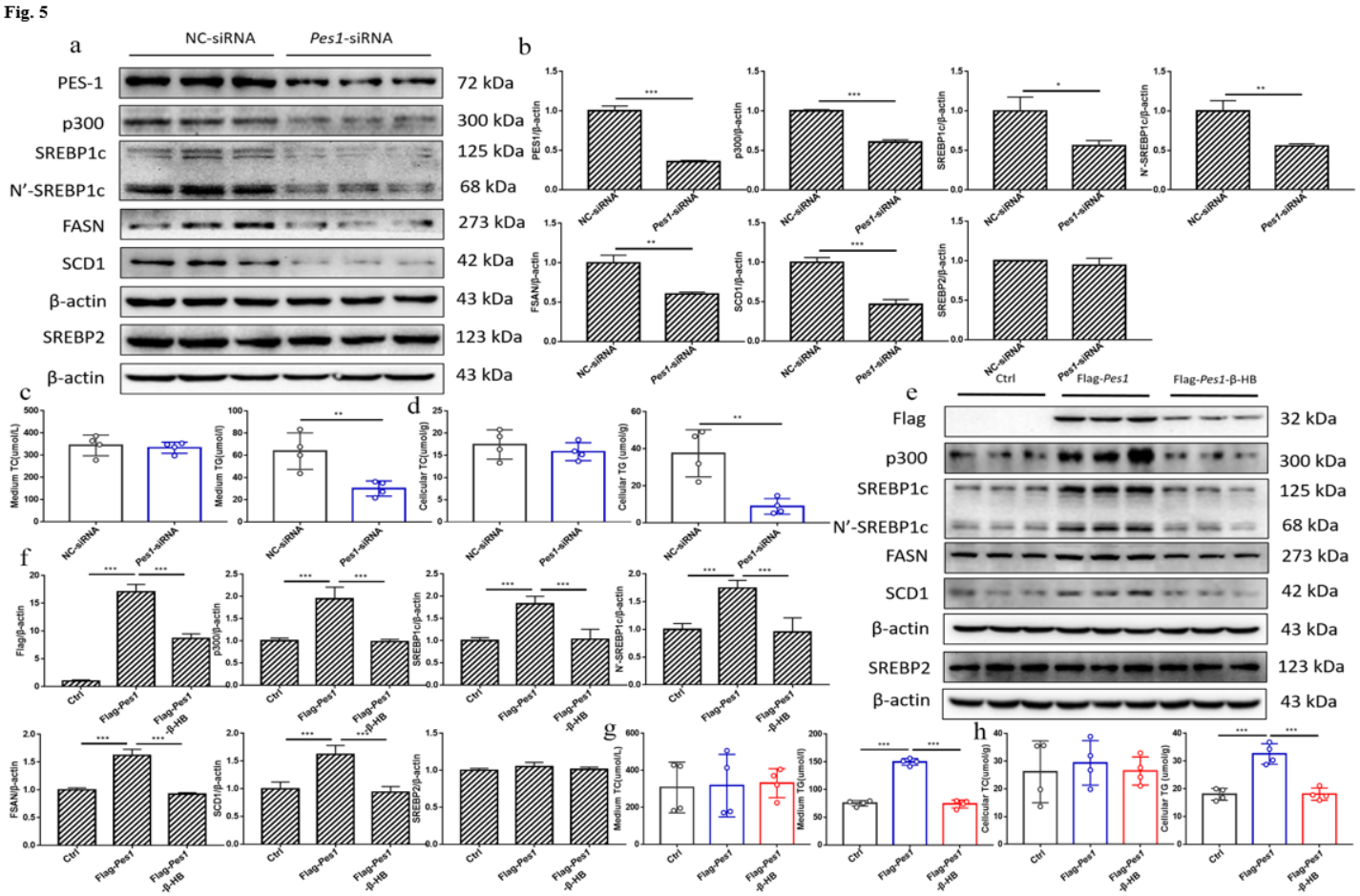

Figure 5

Effects of Pes1 knockdown and overexpression on lipid metabolism in vitro. a-b Pes1 knockdown in cultured liver cells inhibited the protein levels of PES1-Flag, p300, SREBP1c, FASN and SCD1. c-d Displayed are the effects of Pes1 knockdown on the TG and TC levels in cultured liver cells and media. e-f Pes1 overexpression enhanced SREBP1c, p300, FASN and SCD1 protein levels in cultured liver cells, while β-HB treatment abolished the effects. g-h Exhibited are the effects of Pes1 overexpression on the TG and TC levels in cultured liver cells and media. Data were shown as mean ± SEM for each experiment

performed independently 3 times. * P < 0.05, ** P < 0.01, *** P<0.001 compared with controls (Student's t-test or ANOVA, Student-Newman-Keuls q test).

Fig. 6

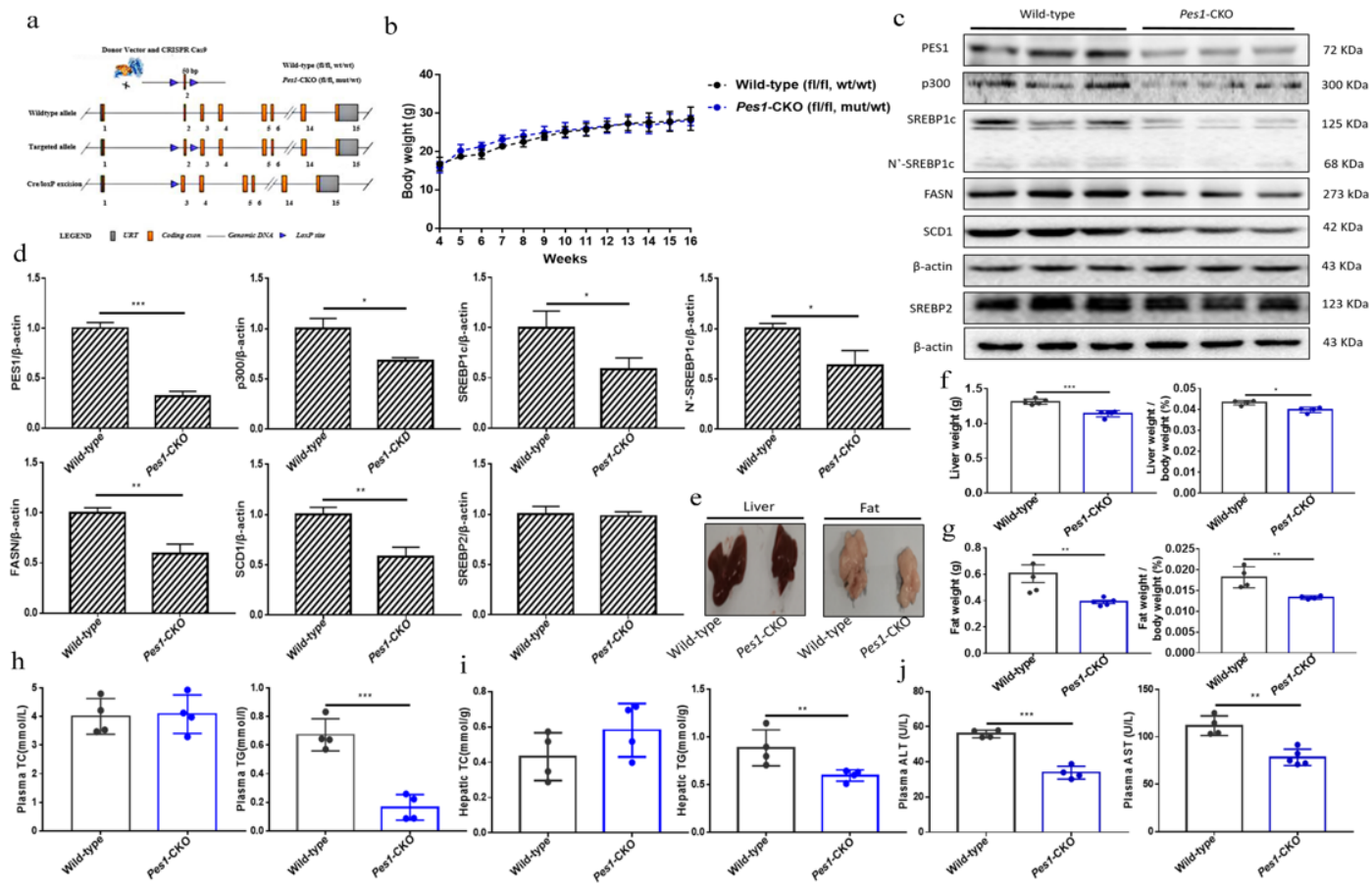

Figure 6

Effects of liver-specific Pes1 knockout on lipid metabolism in vivo. a Displayed is the scheme of Pes1 gene knockout strategy. b Shown are the effects of Pes1 knockout on the murine body weights. c-d Pes1 knockout in mice eliminated the protein levels of PES1, and inhibited p300, SREBP1c, FASN and SCD1 proteins. e-g Shown are the effects of Pes1 knockout on the weights of livers and fat. h-i Demonstrated are the effects of Pes1 knockout on the TG and TC levels in murine plasma and livers. j Plasma AST and ALT levels were measured by Reagent kit. Data were shown as mean ± SEM for each experiment performed independently 3 times. * P < 0.05, ** P < 0.01, *** P<0.001 compared with control (Student's t-test).

Fig. 7

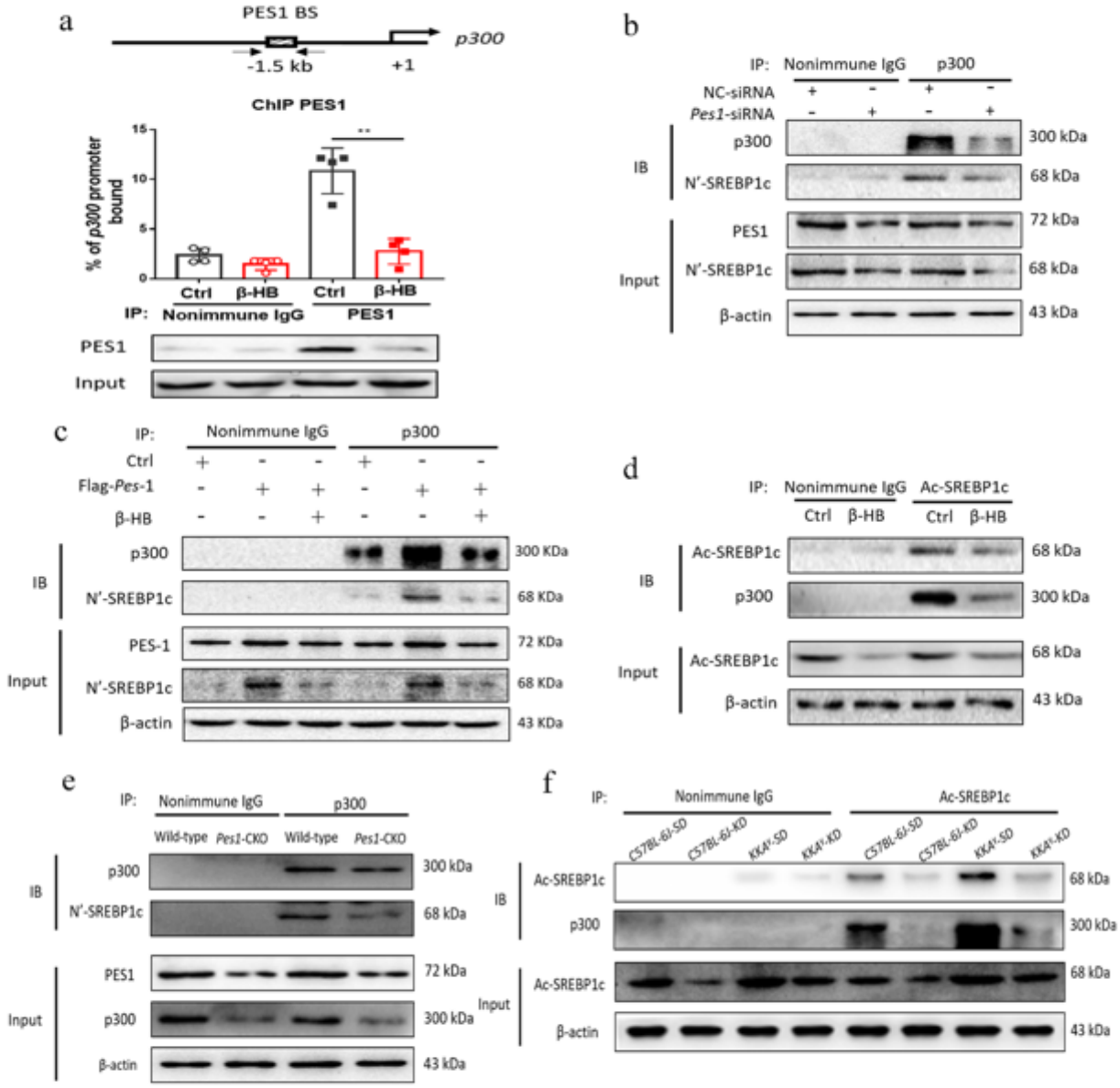

Figure 7

β-HB reduced PES1 binding to the p300 promoter and downregulated PES-1 mediated acetylation of SREBP1c. a β-HB decreased PES1 binding to the p300 promoter. b-c PES1 knockdown or overexpression inhibited or enhanced the interaction between p300 and SREBP1c in hepatocytes. d β-HB treatment decreased the acetylation of SREBP1c in hepatocytes. e Pes1 knockout impaired the interaction between p300 and SREBP1c in mice. f KD feeding decreased the acetylation of SREBP1c in normal and diabetic

mice. Data were shown as mean ± SEM for each experiment performed independently 3 times. * P < 0.05, ** P < 0.01, *** P<0.001 compared with control (ANOVA, Student-Newman-Keuls q test).

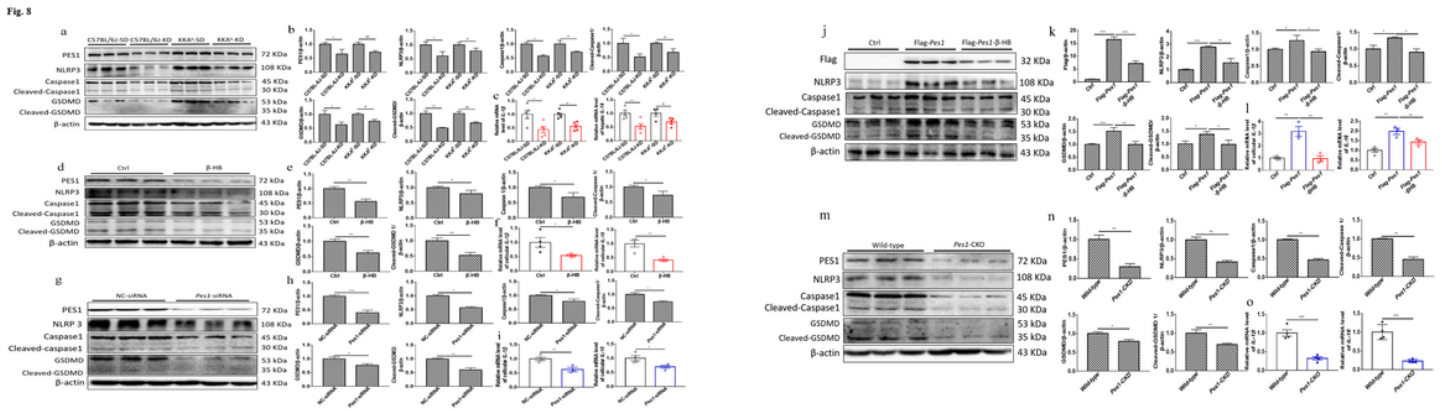

Figure 8

KD feeding and β-HB treatment decreased inflammation responses by downregulating PES1. a-b KD feeding in normal and diabetic mice suppressed the inflammation related proteins. c Relative mRNA levels of hepatic IL-1β and IL-18 were measured by qRT-PCR. d-e β-HB treatment in hepatocytes inhibited the inflammation proteins. f Relative mRNA levels of IL-1β and IL-18 in cultured hepatocytes were measured by qRT-PCR. g-h Pes1 knockdown in hepatocytes lowered the inflammation proteins. i Shown are the effects of Pes1 knockdown on the relative mRNA levels of cellular IL-1β and IL-18. j-k Pes1 supplementation in hepatocytes enhanced the levels of inflammation proteins. l Exhibited are the effects of Pes1 supplementation on the relative mRNA levels of cellular IL-1β and IL-18. m-n Pes1-CKO in mice reduced inflammation proteins in murine livers. o Demonstrated are the effects of Pes1 knockout on the relative mRNA levels of hepatic IL-1β and IL-18. Data were shown as mean ± SEM for each experiment performed independently 3 times. * P < 0.05, ** P < 0.01, *** P<0.001 compared with controls (Student's t-test or ANOVA, Student-Newman-Keuls q test).

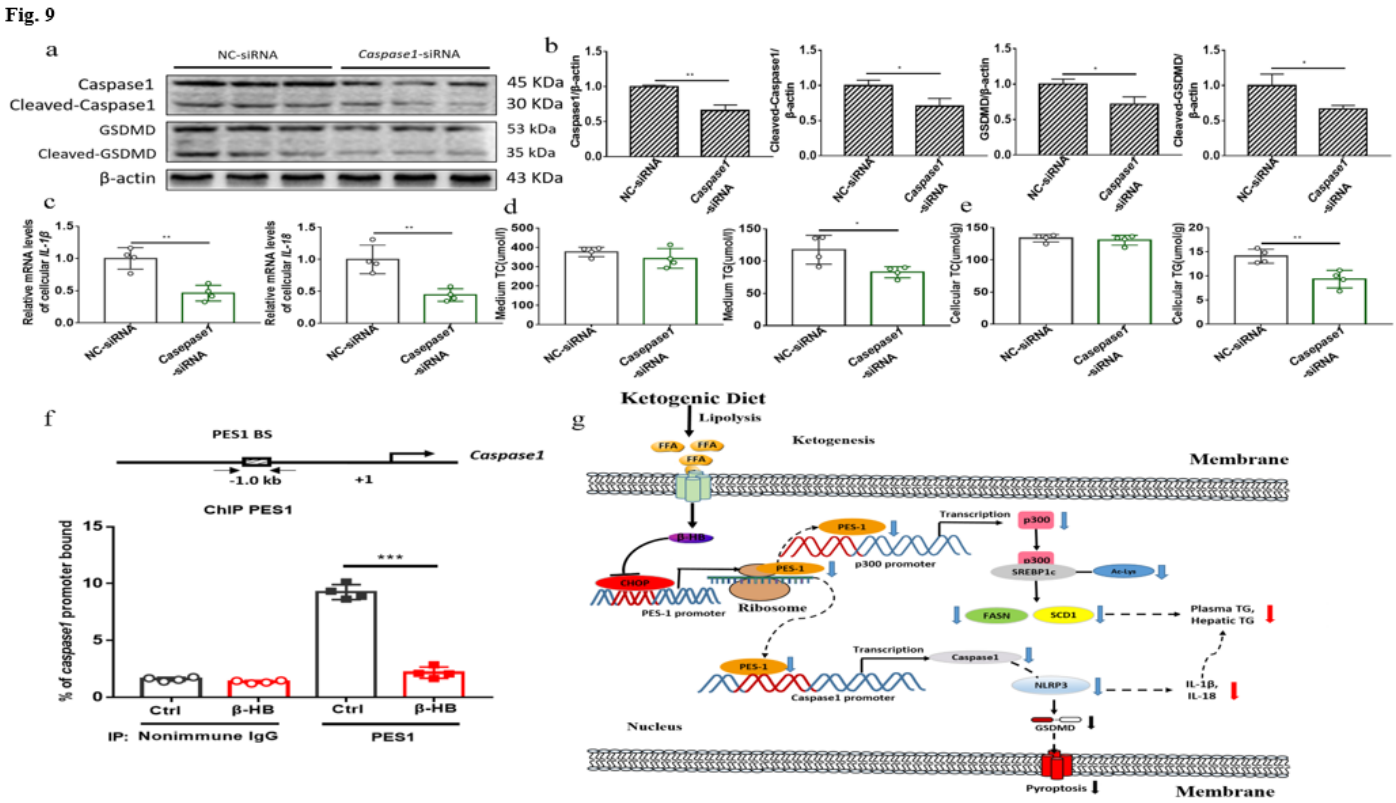

Figure 9

β-HB lowered PES1 binding to the caspase1 promoter and caspase 1 knockdown in hepatocytes reduced the medium and cellular TG. a-b Caspase1 knockdown in liver cells suppressed the inflammation proteins. c Shown are the effects of caspase1 knockdown on the relative mRNA levels of cellular IL-1β and IL-18. d-e Caspase1 knockdown in liver cells reduced the medium and cellular TG. f β-HB decreased PES1 binding to the caspase1 gene promoter. g Schematic diagram of the entire study. Data were shown as mean ± SEM for each experiment performed independently 3 times. * $P < 0.05$, ** $P < 0.01$, *** $P<0.001$ compared with control (ANOVA, Student-Newman-Keuls q test).

Supplementary Files

This is a list of supplementary files associated with this preprint. Click to download.

- SupplementaryMaterial.docx